

High level of stabilized angiostatin mediated by adenovirus delivery does not impair the growth of human neuroblastoma xenografts

Jean-Marc Joseph,^{1,2,a} Céline Bouquet,^{3,a} Paule Opolon,³ Jackie Morizet,¹ Geneviève Aubert,¹ Jochen Rössler,⁴ Nicole Gross,² Frank Griscelli,³ Michel Perricaudet,³ and Gilles Vassal¹

¹UPRES EA3535, Institut Gustave Roussy, 94805 Villejuif, France; ²Laboratoire d'Oncologie Pédiatrique, DMCP, CHUV, 1011 Lausanne, Switzerland; ³UMR 8121 CNRS, Institut Gustave Roussy, 94805 Villejuif, France; and ⁴Universitätsklinikum Essen, 45122 Essen, Germany.

Human neuroblastoma (NB) is a highly heterogeneous childhood cancer secreting a high level of vascular endothelial growth factor (VEGF). Its vascularization has been clearly correlated with metastatic progression and poor outcome. Thus, molecules that target the vascular endothelium are regarded as new therapeutics of clinical interest. Angiostatin, an internal fragment of plasminogen containing the first four kringle structures, has been described as a powerful angiogenic inhibitor. We used a recombinant adenovirus encoding the human angiostatin kringle 1–3 directly fused to human serum albumin HSA (AdK3-HSA). Coupling to HSA has been previously shown to increase the *in vivo* half-life of this angiostatic factor, and to lead to tumor growth inhibition in the MDA-MB-231 carcinoma model. For the assessment of antiangiogenic gene therapy in the human NB IGR-N835 tumor model, 5×10^9 PFU of AdK3-HSA were intravenously injected in tumor-bearing athymic mice presenting either of the following experimental settings: early stage, established, and minimal residual tumors. No delay in tumor growth was observed in animals treated with AdK3-HSA as compared to those treated with the empty virus AdCO1. In early-stage tumors, kinetics of tumor occurrence and tumor growth were similar in AdK3-HSA- and AdCO1-treated animals. K3-HSA was found to be expressed at high levels (the mean value for the three experiments being $19.4 \pm 15.9 \mu\text{g/ml}$) in the circulation of all animals up to 21–35 days after virus injection. In addition, IGR-N835 tumors were found to be highly vascularized and to release high amounts of angiogenic factors, in particular VEGF ($665 \pm 370 \mu\text{g/ml}$ total protein). Thus, in spite of high circulating levels, K3-HSA may be unable to displace the NB proangiogenic switch. In this regard, a more promising target to inhibit NB angiogenesis seems to be the VEGF/VEGFR system.

Cancer Gene Therapy (2003) **10**, 859–866. doi:10.1038/sj.cgt.7700639

Keywords: neuroblastoma; angiostatin; adenovirus; angiogenic balance; children

Neuroblastoma (NB) is one of the most common extracranial solid tumors of infancy and childhood. This highly heterogeneous cancer¹ can form localized tumors (stage 1 or 2), locally invasive tumors (stage 3), or metastatic tumors (stage 4). Prognosis is variable and depends on clinical features and tumor biology, such as histopathology, cellular DNA content, and increased N-myc copy number.² Indeed, amplification of N-myc is a frequent event in advanced stages of human NB (3 and 4), and strongly correlates with poor prognosis.³ Although low-stage tumors are often successfully treated by surgical

resection, high-stage NB is extremely aggressive and usually fatal in older children even after intensive multimodal therapy. NB tumors are initially chemosensitive, in particular to platine, and to temozolomide as more recently reported.^{4,5} However, resistance to chemotherapy is frequently associated with tumor relapses, and little progress has been made to improve the prognosis of patients with high-stage NB tumors. It is therefore important to identify new therapeutic approaches.

Angiogenesis, defined as the formation of new blood capillaries from pre-existing microvessels, is a prerequisite for tumor growth and metastatic dissemination.^{6–8} The onset of angiogenesis in malignancies seems to occur independently of malignant transformation and may develop at various stages during neoplastic development, possibly in conjunction with phenotypic and genotypic changes.^{9–11} Many studies^{12,13} support the concept that

Received February 3, 2003.

Address correspondence and reprint requests to: Dr Gilles Vassal, MD, PhD, Department of Pediatric Oncology, Institut Gustave Roussy, 94805 Villejuif, France. E-mail: gvassal@igr.fr

^aBoth authors contributed equally to this work.

tumor cell growth is controlled by a dynamic balance between angiogenic factors (including vascular endothelial growth factor (VEGF) and basic fibroblast growth factor (bFGF)) and angiostatic factors (such as angiostatin or endostatin). Tumor vascularization has been shown to be associated with clinical outcome in children with NB. Tumor angiogenesis is strongly correlated with metastatic disease, *N-myc* amplification, and decreased survival probability.¹⁴ Furthermore, high-level expression of angiogenic factors (VEGF, b-FGF, angiopoietin 2, TGF- α , PDGF-A, matrix metalloproteinases) is strongly correlated with advanced-stage NB (for a review, see Ribatti et al²). These observations thus suggest that NB might be an attractive target for antiangiogenic therapies in order to switch the balance toward angiostatic factors.

Recent advances in angiogenesis research have highlighted new inhibitors of growth and metastasis of solid tumors. Among the known natural inhibitors of angiogenesis, one of the most potent is angiostatin. Angiostatin, a 38-kDa fragment of plasminogen containing the first four kringle domains, was shown to inhibit specifically endothelial cell proliferation, angiogenesis, and growth of distant pulmonary metastases.¹⁵ Whereas the mechanism of action is unclear, it is known that angiostatin K1–4 and angiostatin-like fragments, such as K1–3, specifically inhibit *in vitro* proliferation of endothelial cells by inducing their apoptosis.^{16,17} Systemic therapy with recombinant angiostatin K1–4 led to the maintenance of metastases in a microscopic dormant state, defined by a balance between apoptosis and proliferation of the tumor cells.^{15,18} Subsequently, it has been shown that angiostatin could also inhibit the growth of primary murine tumors even if the treatment was not initiated until tumors constitute 2% of body weight.¹⁹ Furthermore, resistance to angiostatin has not yet been observed at *in vivo* tested doses up to 100 mg/kg. We have previously demonstrated that intratumoral injection of a replication-defective adenovirus encoding the N-terminal fragment of human plasminogen up to kringle 3 can inhibit primary tumor growth and vascularization in different xenografted tumors.²⁰

Replication-defective adenoviral vectors are indeed particularly well suited for cancer gene therapy as they lead to a transient, but robust, expression of the transgene, and efficient *in vivo* gene transfer has been reported especially in the liver after systemic injection.²¹ Therefore, intravenous injection of a recombinant adenovirus expressing an antiangiogenic factor would induce high-level secretion of this inhibitor, and potentially protect animals from tumor cell establishment and growth.

In the present study, we have investigated the effect of a single intravenous injection of AdK3-HSA in three different experimental situations in nude mice: early stage, advanced, and minimal residual IGR-N835 tumors. Our results failed to demonstrate any efficacy of such an approach in this particular heterotopic highly angiogenic model, despite long-term continuous exposure to the K3-HSA genetic conjugate.

Results

Functional characterization of the K3-HSA conjugate

K1–4 and K1–3 angiostatin fragments were both potent inhibitors of endothelial cell proliferation.^{16,17} To characterize the antiproliferative activity of the K1–3-HSA conjugate expressed from adenovirus, human endothelial HMEC-1 cells were infected for 96 hours at various multiplicities of infection (MOIs) with AdK3-HSA, AdK3, or AdCO1 viruses. The percentage of surviving cells was subsequently determined after incubation with the MTT reagent. Infection with AdK3 and AdK3-HSA viruses resulted in dose-dependent inhibition of endothelial cell proliferation as shown in Figure 1, with survival of 58.1 and 50.6% at MOI 600 with AdK3 and AdK3-HSA respectively, as compared with a 100% survival following AdCO1 infection ($P < .05$, Student's *t*-test). Inhibition of proliferation was specifically linked to the expression of K3 and K3-HSA proteins, as AdCO1 did not affect HMEC proliferation. These results show that the genetic coupling of angiostatin to HSA does not significantly modify its ability to inhibit endothelial cell proliferation.

In vivo evaluation of AdK3-HSA efficacy in the IGR-N835 tumor model

IGR-N835 is derived from a previously treated stage 4 abdominal NB tumor in a 2-year-old boy. A cell line was established from the primary tumor and has been fully characterized.²² The cytogenetic profile of the tumor demonstrates a paradigm mode with a 1:10 translocation and a 11:17 translocation. The mdr 1 gene is not overexpressed as described in a previous report.²³ IGR-N835 exhibits an amplification factor of the *N-myc* oncogene up to 25 copies. The tumor was demonstrated to be tumorigenic after subcutaneous injection of 10^7 cells in nude mice, exhibiting a doubling time of 65 hours.²² The genetic profiles of the parental tumor, the cell line

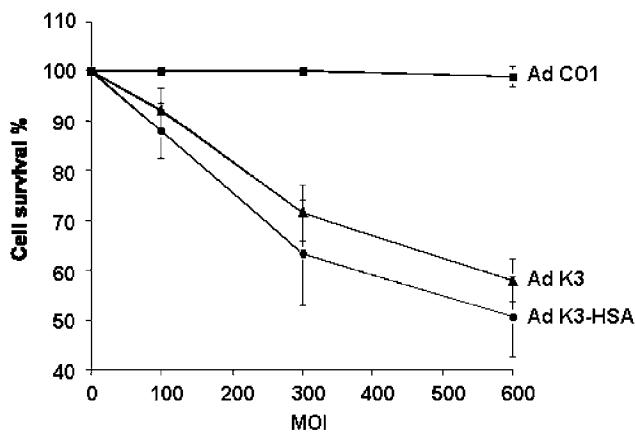


Figure 1 Inhibition of endothelial cell proliferation. Subconfluent HMEC-1 cells were infected at different MOIs for 96 hours with AdK3-HSA (●), AdK3 (▲), and AdCO1 (■).

derived from the tumor (IGR-N835), and the xenografted tumor in nude mice were all identical.

We investigated the effect of a single intravenous injection of AdK3-HSA into the tail vein of nude mice in three different experimental protocols resembling clinical presentations: early stage, advanced, and minimal residual IGR-N835 tumors.

AdK3-HSA evaluation in early-stage tumors. In a first series of experiments, we evaluated AdK3-HSA virus in mice newly engrafted with tumors. At 2 days after tumor implantation, animals were randomly assigned to three groups: (1) control group without treatment (natural history); (2) i.v. injection of 5×10^9 PFU of empty adenovirus (AdCO1); (3) i.v. injection of 5×10^9 PFU of AdK3-HSA. Tumor occurrence was evaluated once a week. No statistical difference was observed between the three experimental groups at day 20 ($P > .05$), day 27 ($P > .1$), day 35 ($P > .2$), and day 42 after virus injection ($P > .5$) (Fig 2). Times to reach 200 mm^3 volume were not statistically different between the three studied groups according to the Kruskal-Wallis statistical test ($P = .396$). The median time to reach a 500 mm^3 volume was 41.3, 42.1, and 44.2 days, and the mean time to reach 500 mm^3 was 44.8 ± 2.6 , 42.2 ± 2.9 , and 48.1 ± 2.7 days, respectively, in groups 1, 2, and 3. Similarly, the median time and mean time to reach 1000 mm^3 volume were not significantly different for the three groups, with 52.5, 49.4, and 51.9 days, and 52.4 ± 2 , 49.8 ± 2.4 , and 55.1 ± 2 days for the mean time, respectively, in groups 1, 2, and 3.

Doubling time was evaluated as the time for the tumors to grow from 200 to 400 mm^3 . The median doubling time was 6, 5, and 6 days, respectively, for the groups 1, 2, and 3, which was not significantly different. Similarly, the

mean time was not significantly different between the three groups with 20.2 ± 4.6 , 17.1 ± 4.5 and 19.6 ± 4.4 days, respectively.

AdK3-HSA evaluation in advanced-stage tumor in association with cisplatin treatment. In a second set of experiments, AdK3-HSA virus was injected in mice bearing pre-established IGR-N835 tumors on the flank. Animals bearing $200 \pm 100 \text{ mm}^3$ tumors were randomly distributed in four groups, and 5×10^9 PFU of AdCO1, or AdK3-HSA, adenoviruses were i.v. injected in association with i.v. cisplatin treatment. In untreated animals, the time to reach a volume above 1000 mm^3 was 24 days. Animals receiving a single injection of 0.2 ml of 0.9% saline solution reached a volume above 1000 mm^3 in 26 days. Animals treated with cisplatin demonstrated 50% of tumor regression. The tumor volumes first decreased from 200 mm^3 to 100 mm^3 at day 14, and then strongly progressed. As shown in Figure 3, tumor growth and the time to reach a volume of 1000 mm^3 (40 days) were identical in both groups injected either with AdK3-HSA (group 3) or AdCO1 (group 4).

AdK3-HSA evaluation in minimal residual tumors obtained after temozolamide treatment. In a last experiment, we addressed the question of whether AdK3-HSA systemic administration was able to delay the tumor relapse after chemotherapeutic treatment. Animals bearing 100 – 300 mm^3 IGR-N835 tumors were treated with temozolamide in order to obtain complete tumor regression. In this experiment design, tumor relapse occurred at day 16. Animals with temozolamide-mediated regressed

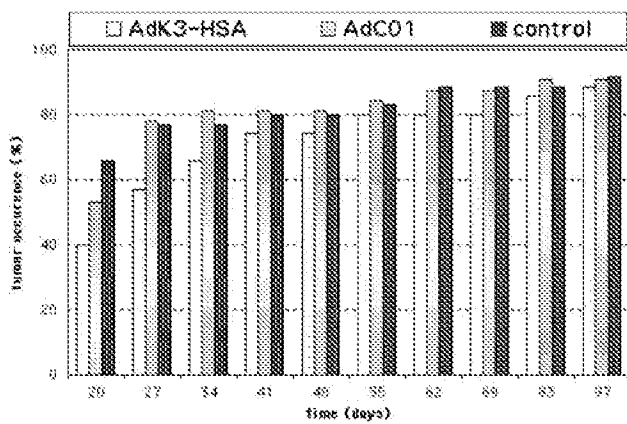


Figure 2 Evaluation of AdK3-HSA systemic treatment in early-stage tumors. At 2 days after tumor graft, animals were randomly assigned to three groups of animals: (1) control group without treatment (natural history; $n=32$); (2) i.v. injection of 5×10^9 PFU of empty adenovirus AdCO1 ($n=35$); (3) i.v. injection of 5×10^9 PFU of AdK3-HSA ($n=35$). Tumor occurrence was evaluated once a week. No statistical difference was observed between the three experimental groups at day 20 ($P > .05$), day 27 ($P > .1$), day 35 ($P > .2$), and day 42 after virus injection ($P > .5$).

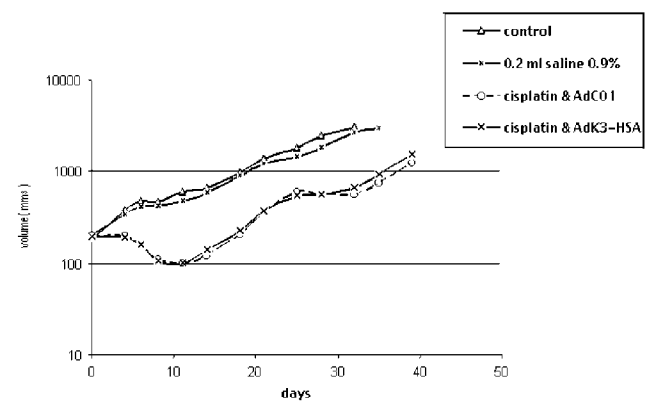


Figure 3 Evaluation of AdK3-HSA systemic treatment in advanced-stage tumors. Animals bearing $200 \pm 100 \text{ mm}^3$ tumors were randomly distributed in four groups ($n=10$ mice/group). The first group did not receive treatment (natural history) and reached a volume $> 1000 \text{ mm}^3$ in 24 days. Animals receiving a single injection of 0.2 ml of 0.9% saline solution reached a volume above 1000 mm^3 in 26 days (group 2). Animals treated with cisplatin demonstrated tumor regression with a volume decrease from 200 to 100 mm^3 at day 14. In total, 5×10^9 PFU of AdCO1 (group 3) or AdK3-HSA (group 4) were i.v. injected in association with an i.v. cisplatin treatment. In both groups (3 and 4) tumor growth was identical, and the time to reach a volume of 1000 mm^3 was 40 days.

tumors were randomly assigned to two groups, and received either (1) a single i.v. injection of 5×10^9 PFU of AdK3-HSA or (2) an i.v. injection of 5×10^9 PFU of AdCO1. Tumor recurrences were identical in both groups. The time to reach a volume of 1000 mm^3 was 56 days after adenovirus injection in both groups (Fig 4).

K3-HSA blood levels after adenovirus injection

In order to confirm the secretion of the K3-HSA conjugate protein into mice blood flow after i.v. injection of the virus, blood samples were collected in the three sets of experiments, and analyzed by ELISA. Following AdCO1 injection, no K3-HSA was detectable in the blood. As shown in Figure 5, high circulating levels of K3-HSA have been measured in the blood of all AdK3-HSA-injected animals. The K3-HSA values were $16.4 \pm 14.5 \mu\text{g/ml}$ in the early-stage group (at day 21 after virus injection), $19.9 \pm 12.0 \mu\text{g/ml}$ in the advanced-stage group (at day 30), and $21.8 \pm 21.3 \mu\text{g/ml}$ in the minimal residual tumor group (at day 35). Thus, in accordance with previous results,²⁴ systemic administration of the AdK3-HSA vector led to a sustained and long-lasting expression of the K3-HSA conjugate in the blood.

Proangiogenic characterization of the IGR-N835 NB tumors

NB tumor progression has been shown to be associated with the expression of angiogenic factors, such as VEGF, and their receptors.^{25,26} High levels of angiogenic factors

(VEGF, b-FGF, angiopoietin 2, TGF- α , PDGF-A) are thus strongly correlated with advanced-stage NB.²

In order to characterize the level of proangiogenic factors released by the IGR-N835 tumor xenografts, 100 mm^3 -IGR-N835 tumors were collected, lysated and analyzed by ELISA for their VEGF content. As we previously reported antitumoral activity of AdK3-HSA on the breast carcinoma MDA-MB-231 model,²⁴ 100 mm^3 -MDA-MB-231 tumors were compared with IGR-N835 tumors. Mice muscles were collected as a negative control. Human VEGF was actually not detected in the muscle samples. The levels of human VEGF in the different tumor samples were $665 \pm 370 \text{ pg}$ of VEGF per mg of protein for the IGR-N835 tumor and $25.1 \pm 1.7 \text{ pg}$ VEGF/mg for the MDA-MB-231 tumor. These data indicate that the human IGR-N835 NB expressed and released very large amounts of the proangiogenic factor VEGF when compared to the breast carcinoma model. After endothelial specific immunochemistry, the IGR-N835 NB was shown to display a typical and important neovascularization, with a dense mass of intratumoral vasculature-associated capillaries, numerous and irregular large-sized veins, and a few arteries (data not shown). Taken together, these observations confirm the strong angiogenic potential of the IGR-N835 NB tumors.

Discussion

The aim of this study was to evaluate the ability of continuous exposure to high serum levels of HSA-

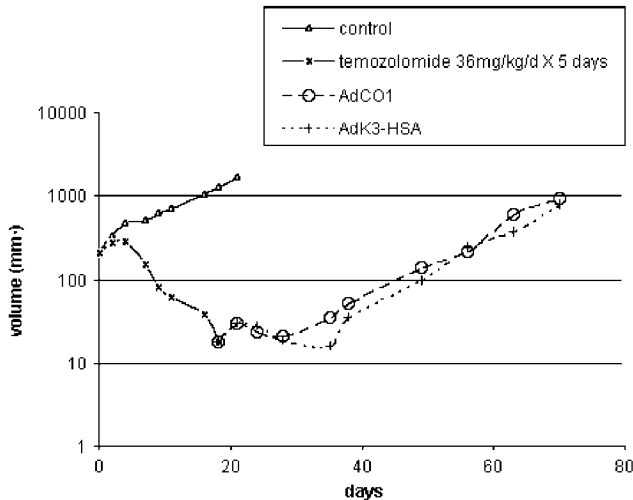


Figure 4 Evaluation of AdK3-HSA systemic treatment in minimal residual tumors. Animals bearing $100-300 \text{ mm}^3$ IGR-N835 tumors were treated with 36 mg/kg/day temozolamide over 5 days in order to obtain complete tumor regression. In this experimental design, tumor relapse occurred toward the 16th day. Animals with regressed tumor were randomly assigned to two groups, and received either (1) a single i.v. injection of 5×10^9 PFU of AdK3-HSA ($n=9$) or (2) an i.v. injection of 5×10^9 PFU of AdCO1 ($n=9$). Tumor recurrences were identical in both groups. The time to reach a volume of 1000 mm^3 was 56 days after adenovirus injection in both groups.

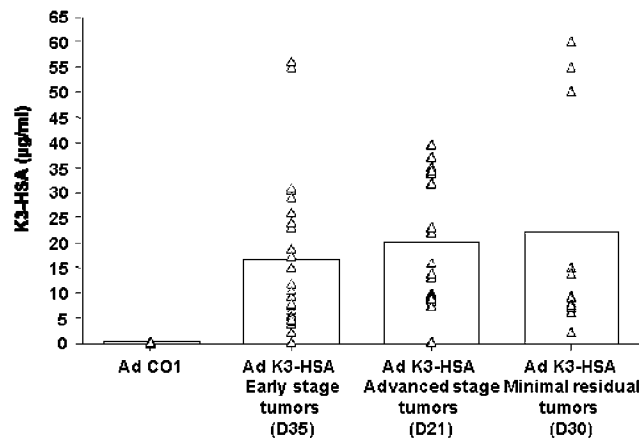


Figure 5 Expression of K3-HSA in treated-mice sera. Sera were collected after a single systemic injection of 5×10^9 PFU of AdK3-HSA adenovirus, at day 21 after virus injection in the early-stage tumors protocol, at day 30 in the advanced-stage tumors protocol, and at day 35 in the minimal residual tumors protocol. K3-HSA blood serum levels were quantified by ELISA using a K1-3 standard (see Materials and methods). No K3-HSA was detectable in the blood after AdCO1 injection. Each triangle represents an individual mouse data point, and the bar graph depicts the mean of data. The K3-HSA values were $16.4 \pm 14.5 \mu\text{g/ml}$ in the early-stage group (day 21), $19.9 \pm 12.0 \mu\text{g/ml}$ in the advanced-stage group (day 30), and $21.8 \pm 21.3 \mu\text{g/ml}$ in the minimal residual tumor group (day 35).

angiostatin K1–3 conjugate to inhibit growth of xenografted human NB. An E1–E3-deleted adenovirus expressing the K3-HSA gene under the control of the early promoter of the cytomegalovirus (CMV) (AdK3-HSA) was used. Systemic injection of this vector (5×10^9 PFU) was performed in three different experimental models of IGR-N835 subcutaneous xenograft in nude mice. First, in the early stage tumor model, adenovirus injection was performed immediately after s.c. xenograft. Then, in the established tumor model (mean tumor volume of 200 mm^3), tumor-bearing animals were treated with a systemic combination of cisplatin and AdK3-HSA. Finally, injection of adenoviruses was performed in mice bearing minimal residual tumors obtained after treatment over a period of 5 days with 36 mg/kg/day temozolomide. Animals with regressed tumors received systemic injection of adenovirus to prevent tumor relapse. In these three different experimental designs, no effect of AdK3-HSA delivery was observed on tumor growth as compared to the AdCO1 groups. In spite of high serum levels of the K3-HSA conjugate in the three experimental groups between 20 and 35 days after virus injection (mean value for the three experiments of $19.4 \mu\text{g K3-HSA/ml}$), no effect on tumor growth and tumor occurrence was observed. The high serum levels obtained in this study confirm the previous observation made by Bouquet et al²⁴ in an MDA-MB-231 human breast cancer model in nude mice.²⁴

Physiological angiogenesis is tightly controlled by a balance between pro- and antiangiogenic factors. In solid tumor growth, a specific clinical turning point is the transition from the avascular to the vascular state, which allows the tumor to grow indefinitely.⁶ During tumor development, high amounts of proangiogenic factors are secreted in the tumor environment leading to the angiogenic switch necessary for neovessel implantation. The aim of an antiangiogenic strategy is to reverse this switch toward the antiangiogenic factors, in order to inhibit tumor vascularization. The efficacy of this strategy has already been proven in various tumor models. Indeed, angiostatin K1–4 and K1–3 angiostatin-like fragments have been shown to inhibit endothelial cell proliferation *in vitro* and tumor angiogenesis *in vivo*.^{19,20} In our study, the HSA conjugate was chosen to improve *in vivo* bioavailability of angiostatin K1–3 after systemic administration. Bouquet et al²⁴ have already shown the benefit of HSA genetic coupling on *in vivo* half-life of angiostatin K1–3 and on MDA-MB-231 tumor growth inhibition. However, a single i.v. injection of AdK3-HSA was inefficient in the NB model. Among antiangiogenic strategies applied to the NB treatment, lack of antitumor activity has already been observed with recombinant endostatin.²⁷ This result was explained by an incorrect folding of the recombinant protein, or an insignificant release of active endostatin from the subcutaneous graft. In our experiments, the use of recombinant adenovirus coding for the K3-HSA gene allows strong and long-lasting expression of functional conjugated angiostatin, as demonstrated by the *in vitro* endothelial cell proliferation assay.

In our model, the lack of antiangiogenic efficacy could be explained by the considerable amounts of proangiogenic factors produced by tumors. These positive regulators are able to stimulate the growth of host's blood vessels. It has been shown that NB tumor progression is mainly associated with expression of angiogenic factors, especially VEGF-A165/121, VEGF-B, and VEGFR-2.^{2,28,29,26} VEGF, a very potent endothelial cell mitogen, may furthermore directly affect NB cell growth and could act as an autocrine growth factor.²⁵ VEGF also upregulates Bcl-2 expression, and significantly protects NB cells from apoptosis *in vitro*.³⁰ Our quantification of VEGF concentration in the IGR-N835 NB tumor demonstrates a VEGF level 26-fold higher than that observed in MDA-MB-231 control breast tumors. Furthermore, PECAM-1 immunohistochemistry, specific for endothelial cells, highlights a strong and early angiogenic feature of NBs with dense intratumoral vasculature, large-sized veins, and few arteries (data not shown). Taken together, and in comparison with the MDA-MB-231 study, these results suggest that the high serum levels of K3-HSA obtained after systemic administration of the adenovirus vector were probably not able to counterbalance the very high level of VEGF released by the IGR-N835 tumors. Ambs et al³¹ have shown that inhibition of B16F10 tumor growth correlates with expression level of human angiostatin. They first demonstrated that high angiostatin expression levels were needed to achieve tumor remission.³¹ This observation suggests that anti-angiogenic gene transfer requires high expression levels of the therapeutic factor in order to switch the angiogenic balance off. Each tumor cell line would be characterized by its specific positive/negative angiogenic secretion levels. We hypothesize that antiangiogenic factors should have to be expressed beyond a tumor-specific threshold in order to inhibit angiogenesis and tumor growth efficiently. Our results strengthen this hypothesis: where $20 \mu\text{g/ml}$ of circulating K3-HSA is sufficient to counterbalance 25 pg of VEGF per mg of MDA-MB-231 tumor proteins, this inhibitor level is clearly inefficient against 665 pg of VEGF per mg of IGR-N835 tumor proteins. Moreover, the bFGF level is only 1.7-fold higher in the NB tumor *versus* the breast carcinoma (data not shown), suggesting that this factor plays only a modest role in the lack of antitumor efficacy. Taken together, these observations indicate that angiostatin, despite its known potent antitumor activity, is not sufficient *per se* to treat NB tumors. The more promising target to inhibit NB angiogenesis seems therefore to be the VEGF/VEGFR system, as demonstrated by several studies. Klement et al³² showed a full and sustained regression of large NB tumors after continuous low-dose therapy with vinblastine associated with an antibody directed against the receptor VEGFR-2. Kim et al³³ also obtained a significant inhibition of NB xenograft growth with chemotherapy (topotecan, a topoisomerase-I inhibitor) combined with anti-VEGF antibody.³³ Anti-VEGF gene transfer strategies have also been developed, employing *ex vivo* infection by a recombinant retrovirus.^{34,28} These results suggest that neutralization of proangiogenic factors, such as

VEGF, should be considered. To this end, association of an adenovirus expressing the soluble fragment of Flk-1 with AdK3-HSA should efficiently antagonize angiogenesis in highly vascularized tumors releasing large amounts of VEGF such as IGR-N835 NB.

Materials and methods

Adenoviral construct

Ad K3-HSA is a Δ E1– Δ E3 recombinant adenovirus expressing the K3-HSA gene under the control of the CMV immediate-early promoter. This genetic conjugate consists of a fragment comprising the 18-amino-acid (aa) native secretion signal followed by the first 326 residues of human plasminogen (angiostatin Kringle 1–3) directly linked to a DNA fragment encoding the 585 residues of mature HSA.²⁴ Recombinant adenovirus that did not encode the transgene (Ad CO1) was used as negative control in this study. Viral stocks were prepared on HEK 293 cells and purified twice on CsCl gradients. Desalting was performed using Pharmacia G50 columns (Orsay, France), and viruses were frozen in phosphate-buffered saline (PBS)–10% glycerol at –80°C. Titers were calculated as plaque forming unit/ml (PFU/ml) on 911 cells.³⁵

Proliferation assay

Subconfluent HMEC-1 cells were infected at different MOIs with AdK3-HSA, AdK3, or AdCO1 in 24-well culture plates for 96 hours. Supernatants were then discarded and cells were incubated with 250 μ l of PBS and 25 μ l of MTT (Sigma) at 5 mg/ml. After a 2-hour incubation at 37°C, 250 μ l of lysis buffer (20% SDS–33% dimethylformamide–2% acetic acid–0.025 N HCl–0.05 N NaOH) was added and incubated overnight. A measure of 200 μ l of each sample was distributed in 96-well plates for an optical density reading at 570 nm.

In vivo experiments

All animal experiments were conducted with athymic Swiss nude mice locally bred, in accordance with the European Community guidelines (directive no. 86/609/CEE). Treatment was initiated when the tumors reached 100–300 mm³. Two tumor perpendicular diameters were measured twice per week and each individual tumor volume calculated according to the equation: V (mm³) = d^2 (mm²) $\times D$ (mm)/2, where d and D are the smallest and largest tumor diameters, respectively. The treatments were pursued until tumor volumes reached a size of 1500–2000 mm³. *In vivo* treatment efficacy was evaluated in advanced-stage tumor models according to the method previously described.²³

Early-stage tumor

Animals were engrafted with tumor fragments of 15 mm³, randomly assigned to three groups, and treated 2 days after tumor engraftment: (1) control group without treatment (natural history; n = 32); (2) i.v. injection of

5 \times 10⁹ PFU of empty adenovirus AdCO1 into the tail vein of mice (n = 35); (3) i.v. injection of 5 \times 10⁹ PFU of Ad-K3-HSA (n = 35). Tumor occurrence was evaluated every week starting at day 20. Delay to reach a volume of 200 mm³, time to grow from 200 to 400 mm³, and time to reach 500 and 1000 mm³ tumor volumes were evaluated in all groups.

Advanced-stage tumors

At 3 weeks after tumor engraftment, animals bearing 200 \pm 100 mm³ tumors were randomly assigned to four experimental groups (n = 10 animals/group): (1) control group without treatment (natural history); (2) i.v. injection of 0.2 ml of NaCl 0.9% into the tail vein of mice; (3) i.v. injection of 14 mg/kg cisplatin followed by i.v. injection of 5 \times 10⁹ PFU of AdCO1; (4) i.v. injection of 14 mg/kg cisplatin followed by 5 \times 10⁹ PFU of Ad-K3-HSA. The antitumor activity end point was evaluated in terms of tumor growth (TG). Complete regression (CR) was defined as regression beyond the palpable limit (15 mm³), and partial regression (PR) as a regression over 50% of the initial tumor volume. CR and PR had to be observed for at least two consecutive tumor measurements in order to be retained. Tumor growth delay (TGD) was defined as the difference in the median times between the treated group and the control group to reach a tumor volume that was five times greater than the initial tumor volume. Tumor-free survival (TFS) was defined as an animal free of measurable tumor more than 4 months after treatment. The activity of the K3-HSA adenoviral treatment was evaluated in term of TG, TGD, TFS, PR, and CR.

Minimal residual tumors

At 3 weeks after tumor graft, animals bearing 100–300 mm³ tumors were randomly assigned to five groups (n = 6/group). Four groups of animals received 36 mg/kg/day p.o. temozolomide suspended in 0.2 ml of klucel over a period of 5 days. The last group of animals received 0.2 ml of klucel over a period of 5 days. Tumor volumes were measured every day.

At day 14, after initiating the treatment with temozolomide, animals with complete regressed tumors were randomly assigned to two groups: (1) i.v. injection of 5 \times 10⁹ PFU of Ad-K3-HSA (n = 9) and (2) i.v. injection of 5 \times 10⁹ PFU of AdCO1 (n = 9). The activity of the K3-HSA adenoviral treatment was evaluated in terms of tumor growth and time to reach a 100-mm³ volume.

K3-HSA blood levels assay

For the three different experimental groups, blood samples were collected 21, 30, or 35 days after virus injection. Sera were analyzed by a sandwich enzyme-linked immunosorbent assay (ELISA) to quantify the K3-HSA circulating levels. The 96-well microtiter plates (Nunc Maxisorb, Roskilde, Denmark) were coated with 100 μ l of goat anti-human angiostatin antibody (AF226, R&D Systems Inc., Minneapolis, MN) diluted to 1 μ g/ml

in PBS. After overnight incubation at 4°C, the wells were washed six times with TBST (Tris-buffered saline (TBS), 0.02% Tween-20 (Sigma, France)) and then incubated with TBST-5% non-fat dry milk powder (Regilait, Nestlé, France). Wells were blocked with 200 µl of TBST-5% milk for 2 hours at room temperature on a rocking platform shaker. After washing as above, wells were incubated in TBST with serial dilutions of mice sera or standard human angiostatin K1-3 (ref. 176705, Calbiochem, La Jolla, CA). After 2 hours of incubation with shaking and washing as above, the wells were incubated with 50 µl of mouse antihuman angiostatin antibody (528176, Calbiochem, San Diego, CA) diluted to 500 ng/ml in TBST-5% milk. After incubation and washing as described above, wells were incubated with 50 µl of an alkaline phosphatase-conjugated goat anti-mouse IgG (H + L) antibody (S3721, Promega, Madison, WI) diluted to 1:5000 in TBST-5% milk. After 1 hour of incubation and washing as above, K3-HSA was detected by a 30-minute incubation with developing solution (alkaline phosphatase substrate kit; Bio-Rad Laboratories, Richmond, CA). The absorbance at 405 nm (A_{405}) was measured using a microplate reader (Bio-Rad).

VEGF ELISA

IGR-N835 and MDA-MB-231 tumor fragments were harvested from 100 mm³ tumors, and subsequently snap frozen in liquid N₂. Nude mice muscle tissue was used as a negative control. The tissue fragments were cut into small pieces and suspended in 300 µl PBS containing 10% protease inhibitors (Roche Diagnostics GmbH, Mannheim, Germany). Sonication was performed for 30 minutes followed by centrifugation for 20 minutes at 14,000 rpm. Supernatants were assayed for protein and cytokine content. Total protein amount was quantified using the Bradford method (Biorad Laboratories, Richmond, CA). Human VEGF levels were measured by ELISA kits (R&D Systems Inc., Minneapolis, MN) in duplicates according to the manufacturer's instructions, and the mean values were calculated.

Acknowledgments

We thank Patrice Arduouin and the staff of the animal care unit at the Institut Gustave Roussy. We also thank Lysiane Laudani (UPRES EA3535) and Elisabeth Connaught (UMR 8121) for their technical assistance. La Ligue Nationale contre le Cancer, l'Association pour la Recherche contre le Cancer (ARC), and le Centre National de la Recherche Scientifique (CNRS) are acknowledged for financial support.

References

- Brodeur GM. Molecular basis for heterogeneity in human neuroblastomas. *Eur J Cancer*. 1995;31A:505-510.
- Ribatti D, Vacca A, Nico B, De Falco G, Giuseppe MP, Ponzoni M. Angiogenesis and anti-angiogenesis in neuroblastoma. *Eur J Cancer*. 2002;38:750-775.
- Brodeur GM, Fong CT. Molecular biology and genetics of human neuroblastoma. *Cancer Genet Cytogenet*. 1989;41:153-174.
- Houghton PJ, Stewart CF, Cheshire PJ, Richmond LB, Kirstein MN, Poquette CA, Tan M, Friedman HS, Brent TP. Antitumor activity of temozolomide combined with irinotecan is partly independent of O₆-methylguanine-DNA methyltransferase and mismatch repair phenotypes in xenograft models. *Clin Cancer Res*. 2000;6(10):4110-4118.
- Middlemas DS, Stewart CF, Kirstein MN, Poquette C, Friedman HS, Houghton PJ, Brent TP. Biochemical correlates of temozolomide sensitivity in pediatric solid tumor xenograft models. *Clin Cancer Res*. 2000;6:998-1007.
- Folkman J. The role of angiogenesis in tumor growth. *Semin Cancer Biol*. 1992;3:65-71.
- Weidner N, Semple JP, Welch WR, Folkman J. Tumor angiogenesis and metastasis — correlation in invasive breast carcinoma. *N Engl J Med*. 1991;324:1-8.
- Weidner N. Intratumor microvessel density as a prognostic factor in cancer. *Am J Pathol*. 1995;147:9-19.
- Folkman J, and Shing Y. Angiogenesis. *J Biol Chem*. 1992;267:10931-10934.
- Liotta LA, Stetler-Stevenson WG. Tumor invasion and metastasis: an imbalance of positive and negative regulation. *Cancer Res*. 1991;51(18 Suppl):5054s-5059s.
- Weinstat-Saslow D, Steeg PS. Angiogenesis and colonization in the tumor metastatic process: basic and applied advances. *FASEB J*. 1994;8:401-407.
- Rastinejad F, Polverini PJ, Bouck NP. Regulation of the activity of a new inhibitor of angiogenesis by a cancer suppressor gene. *Cell*. 1989;56:345-355.
- Good DJ, Polverini PJ, Rastinejad F, Le Beau MM, Lemons RS, Frazier WA, Bouck NP. A tumor suppressor-dependent inhibitor of angiogenesis is immunologically and functionally indistinguishable from a fragment of thrombospondin. *Proc Natl Acad Sci USA*. 1990;87(17):6624-6628.
- Meitar D, Crawford SE, Rademaker AW, Cohn SL. Tumor angiogenesis correlates with metastatic disease, N-myc amplification, and poor outcome in human neuroblastoma. *J Clin Oncol*. 1996;14:405-414.
- O'Reilly MS, Holmgren L, Shing Y, Chen C, Rosenthal RA, Moses M, Lane WS, Cao Y, Sage EH, Folkman J. Angiostatin: a novel angiogenesis inhibitor that mediates the suppression of metastases by a Lewis lung carcinoma. *Cell*. 1994;79:315-328.
- Cao Y, Ji RW, Davidson D, Schaller J, Marti D, Sohndel S, McCance SG, O'Reilly MS, Llinas M, Folkman J. Kringle domains of human angiostatin. Characterization of the anti-proliferative activity on endothelial cells. *J Biol Chem*. 1996;271(46):29461-29467.
- Lucas R, Holmgren L, Garcia I, Jimenez B, Mandriota SJ, Borlat F, Sim BK, Wu Z, Grau GE, Shing Y, Soff GA, Bouck N, Pepper MS. Multiple forms of angiostatin induce apoptosis in endothelial cells. *Blood*. 1998;92(12):4730-4741.
- Holmgren L, O'Reilly MS, Folkman J. Dormancy of micrometastases: balanced proliferation and apoptosis in the presence of angiogenesis suppression. *Nat Med*. 1995;1:149-153.
- O'Reilly MS, Holmgren L, Chen C, Folkman J. Angiostatin induces and sustains dormancy of human primary tumors in mice. *Nat Med*. 1996;2:689-692.

20. Griselli F, Li H, Bennaceur-Griselli A, Soria J, Opolon P, Soria C, Perricaudet M, Yeh P, Lu H. Angiostatin gene transfer: inhibition of tumor growth *in vivo* by blockage of endothelial cell proliferation associated with a mitosis arrest. *Proc Natl Acad Sci USA*. 1998;95:6367–6372.

21. Kass-Eisler A, Falck-Pedersen E, Elfenbein DH, Alvira M, Buttrick PM, Leinwand LA. The impact of developmental stage, route of administration and the immune system on adenovirus-mediated gene transfer. *Gene Therapy*. 1994;1:395–402.

22. Bettan-Renaud L, Bayle C, Teyssier JR, Benard J. Stability of phenotypic and genotypic traits during the establishment of a human neuroblastoma cell line, IGR-N-835. *Int J Cancer*. 1989;44:460–466.

23. Vassal G, Terrier-Lacombe MJ, Bissery MC, Venuat AM, Gyergyay F, Benard J, Morizet J, Boland I, Arduin P, Bressac-de-Paillerets B, Gouyette A. Therapeutic activity of CPT-11, a DNA-topoisomerase I inhibitor, against peripheral primitive neuroectodermal tumour and neuroblastoma xenografts. *Br J Cancer*. 1996;74:537–545.

24. Bouquet C, Frau E, Opolon P, Connault E, Abitbol M, Griselli F, Yeh P, Perricaudet M. Systemic administration of a recombinant adenovirus encoding a HSA-angiostatin kringle 1–3 conjugate inhibits MDA-MB-231 tumor growth and metastasis in a transgenic model of spontaneous eye cancer. *Mol Ther*. 2003;7:174–184.

25. Langer I, Vertogen P, Perret J, Fontaine J, Atassi G, Robberecht P. Expression of vascular endothelial growth factor (VEGF) and VEGF receptors in human neuroblastomas. *Med Pediatr Oncol*. 2000;34:386–393.

26. Komuro H, Kaneko S, Kaneko M, Nakanishi Y. Expression of angiogenic factors and tumor progression in human neuroblastoma. *J Cancer Res Clin Oncol*. 2001;127:739–743.

27. Jouanneau E, Alberti L, Nejjari M, Treilleux I, Vigrain I, Duc A, Combaret V, Favrot M, Leboulch P, Bachelot T. Lack of antitumor activity of recombinant endostatin in a human neuroblastoma xenograft model. *J Neurooncol*. 2001;51:11–18.

28. Davidoff AM, Leary MA, Ng CY, Vanin EF. Gene therapy-mediated expression by tumor cells of the angiogenesis inhibitor flk-1 results in inhibition of neuroblastoma growth *in vivo*. *J Pediatr Surg*. 2001;36:30–36.

29. Rossler J, Breit S, Havers W, Schweigerer L. Vascular endothelial growth factor expression in human neuroblastoma: up-regulation by hypoxia. *Int J Cancer*. 1999;81:113–117.

30. Beirle EA, Strande LF, Chen MK. VEGF upregulates Bcl-2 expression and is associated with decreased apoptosis in neuroblastoma cells. *J Pediatr Surg*. 2002;37:467–471.

31. Ambs S, Dennis S, Fairman J, Wright M, Papkoff J. Inhibition of tumor growth correlates with the expression level of a human angiostatin transgene in transfected B16F10 melanoma cells. *Cancer Res*. 1999;59:5773–5777.

32. Klement G, Baruchel S, Rak J, Man S, Clark K, Hicklin DJ, Bohlen P, Kerbel RS. Continuous low-dose therapy with vinblastine and VEGF receptor-2 antibody induces sustained tumor regression without overt toxicity [see comments]. *J Clin Invest*. 2000;105(8):R15–R24. [Comment in: *J. Clin Invest*. 2000;105:1045–1047].

33. Kim ES, Soffer SZ, Huang J, McCrudden KW, Yokoi A, Manley CA, Middlesworth W, Kandel JJ, Yamashiro DJ. Distinct response of experimental neuroblastoma to combination antiangiogenic strategies. *J Pediatr Surg*. 2002;37:518–522.

34. Davidoff AM, Leary MA, Ng CY, Vanin EF. Retroviral vector-producer cell mediated angiogenesis inhibition restricts neuroblastoma growth *in vivo*. *Med Pediatr Oncol*. 2000;35:638–640.

35. Fallaux FJ, Kranenburg O, Cramer SJ, Houwelling A, Van Ormondt H, Hoeben RC, Van Der Eb AJ. Characterization of 911: a new helper cell line for the titration and propagation of early region 1-deleted adenoviral vectors. *Hum Gene Ther*. 1996;7:215–222.